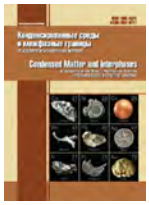

ISSN 1606-867X (Print)
ISSN 2687-0711 (Onine)
Condensed Matter and Interphases
Kondensirovannye Sredy i Mezhfaznye Granitsy
https://journals.vsu.ru/kcmf/

Original articles

Original article
https://doi.org/10.17308/kcmf.2021.23/3300

Features of the two-stage formation of macroporous and mesoporous silicon structures

A. S. Lenshin✉, A. N. Lukin, Ya. A. Peshkov, S. V. Kannykin, B. L. Agapov, P. V. Seredin, E. P. Domashevskaya

Voronezh State University,
1 Universitetskaya pl., Voronezh 394018, Russian Federation

Abstract

The aim of this work was the formation of multilayer structures of macroporous silicon and the study of their structural, morphological, and optical properties in comparison with the properties of multilayer structures of mesoporous silicon.

The paper presents the results of the development of techniques for the formation of multilayer structures of porous silicon *por*-Si by stepwise change in the current with two-stage modes of electrochemical etching.

The data on the morphology, composition, and porosity of macroporous and mesoporous silicon samples were obtained using scanning electron microscopy, IR spectroscopy, and X-ray reflectivity. It was shown that with the two-stage growth of porous silicon layers, the depth of the boundary between the layers of the structure was determined by the primary mode of electrochemical etching, while the total layer thickness increased with an increase in the current density of electrochemical etching.

A comparative analysis of the relative intensity and fine structure of vibrational modes of IR spectra indicated a significantly more developed specific pore surface and greater sorption capacity of mesoporous silicon as compared to macroporous silicon.

Keywords: macroporous silicon, mesoporous silicon, electrochemical etching, porosity, IR spectra, X-ray reflectivity

Acknowledgements: The study was supported by the Russian Foundation for Basic Research and the Government of the Voronezh Region in the framework of the scientific project No. 19-42-363004. The work on the development of techniques for the formation of porous silicon layers with different porosity was carried out with the financial support of the Russian Science Foundation grant 19-72-10007. This work was partially supported by the Ministry of Science and Higher Education of the Russian Federation within the framework of the state assignment to universities in the field of scientific activity for 2020-2022, project No. FZGU-2020-0036. The studies were conducted in the Centre for Collective Use of Scientific Equipment of Voronezh State University (http://ckp.vsu.ru).

For citation: Lenshin A. S., Lukin A. N., Peshkov Ya. A., Kannykin S. V., Agapov B. L., Seredin P. V., Domashevskaya E. P. Features of two-stage formation of macroporous and mesoporous silicon structures. *Kondensirovannye sredy i mezhfaznye granitsy = Condensed Matter and Interphases.* 2021; 23 (1): 41–49. https://doi.org/10.17308/kcmf.2021.23/3300

Для цитирования: Леньшин А. С., Лукин А. Н., Пешков Я. А., Канныкин С. В., Агапов Б. Л., Середин П. В., Домашевская Э. П. Особенности двухстадийного формирования структур макропористого и мезопористого кремния. *Конденсированные среды и межфазные границы.* 2021;23(1): 41-48. https://doi.org/10.17308/kcmf.2021.23/3300

✉ Alexander S. Lenshin, e-mail: lenshinas@phys.vsu.ru

1. Introduction

The use of porous silicon *por*-Si as one of the materials of modern solid-state functional electronics is due to the presence of many practically useful functional properties of this material and its compatibility with most technological production processes. It is known that depending on the method of its production, *por*-Si can have an extremely large area of specific surface of pores (up to 500 m^2/g), high reactivity, and intense photoluminescence (PL) in the visible range of wavelengths [1–4].

Previously in the 20th century, before the concept of "nano" and the nanoscopic scale were introduced into scientific terminology, according to the IUPAC classification, pores with a radius of up to 0.2 nm were called submicropores, pores with a radius of 0.2–1.0 nm were called micropores, pores with a radius of 1–25 nm were called mesopores, and those with a radius of more than 25 nm were called macropores [5]. Currently there are different variants of systematisation of porous materials by their morphology and physicochemical properties. Regardless of the size of the pores, porous silicon is usually characterised by such parameter as "porosity" *P*, which is the ratio of the volume of pores to the total volume of the porous layer of the sample, as well as by the average size of the structural elements. With a low value of porosity, the properties of *por*-Si are similar to the properties of crystal silicon, although they can change if the value increases. For instance, photoluminescence was found in the samples of *por*-Si with a value of porosity of at least 50 % [6].

Depending on the initial material, porosity, and formation conditions, porous silicon has a wide range of values of resistivity (10^{-2}–10^{11} Ohm·cm), absolute permittivity (1.75–12), and refractive index (1.2–3.5) [7]. In a number of works [1–4] it is shown that changes in the modes of formation of *por*-Si and post-processing of its surface allow effectively controlling the morphology, surface composition, and optical and adsorption properties of *por*-Si [6].

The possibilities of creating gas sensors, optical sensors, and moisture sensors were demonstrated on the structures of porous silicon. The use of multi-stage modes of formation of a porous layer on single-crystal silicon can also be promising for fine adjustment of the functional properties of its surface and volume for the further formation of thin layers of such modern nanoelectronic materials as metal oxide structures or structures of the A3B5 type on its surface [1–4, 8–10].

The aim of this work was the study of multilayer structures of macroporous silicon and their structural, morphological, and optical characteristics in comparison with the characteristics of multilayer structures of mesoporous silicon that we previously obtained [11].

2. Experimental

Multilayer structures of porous silicon (henceforth referred to as "macroporous silicon") were formed on the surface of crystal silicon substrates *c*-Si (100) with a resistivity of 0.3 Ohm·cm, doped with phosphorus. Electrochemical etching (ECE) was performed in a solution of hydrofluoric acid and dimethylformamide with the addition of hydrogen peroxide and sulphuric acid while periodically changing the current density. At the same time, the current density gradually changed during the process of the two-stage ECE. The modes of electrochemical etching are presented in table 1.

The samples were obtained in the modes similar to those that were used to synthesise the samples of mesoporous silicon in our previous work [11]. Only the composition of the ECE solution was changed towards a lower content of hydrofluoric acid. The morphological features of the samples were studied using scanning electron microscopy SEM (JEOL JSM 6380 LV).

Table 1. Conditions for obtaining the samples of porous silicon

No.	Etching mode	Anodic current density, mA/cm^2	Etching time, minutes
1	single-stage	15	10
2	single-stage	50	10
3	two-stage	50/15	5/5
4	two-stage	15/50	5/5

IR spectra of multilayer structures were obtained on a Vertex 70 (Bruker) IR Fourier spectrometer using an attachment for disturbed total internal reflection (ATR) spectroscopy [9] in the range of 400–4000 cm^{-1}. IR spectra were collected two weeks after the samples had been obtained.

To determine the porosity of the surface layer of *por*-Si with the thickness of 10 nm, the samples obtained using single-stage ECE were studied using X-ray reflectivity (XRR) on a laboratory diffractometer ARL X'TRA (Cu *K*α) with Bragg-Brentano geometry within a small angle range of (2θ = 0.1–1°).

3. Results and discussion

3.1. Structural and morphological SEM data

Figure 1 presents SEM microphotographs of cleavages of macroporous *por*-Si samples with an average diameter of the main type of pores of approximately 150–200 nm obtained in single-stage and two-stage ECE modes with the following anodic current densities: 15 mA/cm^2 (No. 1) and 50 mA/cm^2 (No. 2), 50/15 mA/cm^2 (No. 3) and15/50 mA/cm^2 (No. 4).

The analysis of the SEM data shows that an increase in the current density in the specified range causes an increase in the thickness of the porous layer and in the size of the pores, but, unlike mesoporous silicon [11] obtained with the same ECE modes (Fig. 2), there is no partial cracking of the porous layer, and the boundary between the porous layers is less pronounced. For example, the thickness of the porous layer of sample No. 1 obtained using a single-stage mode with the current density of j = 15 mA/cm^2 was~

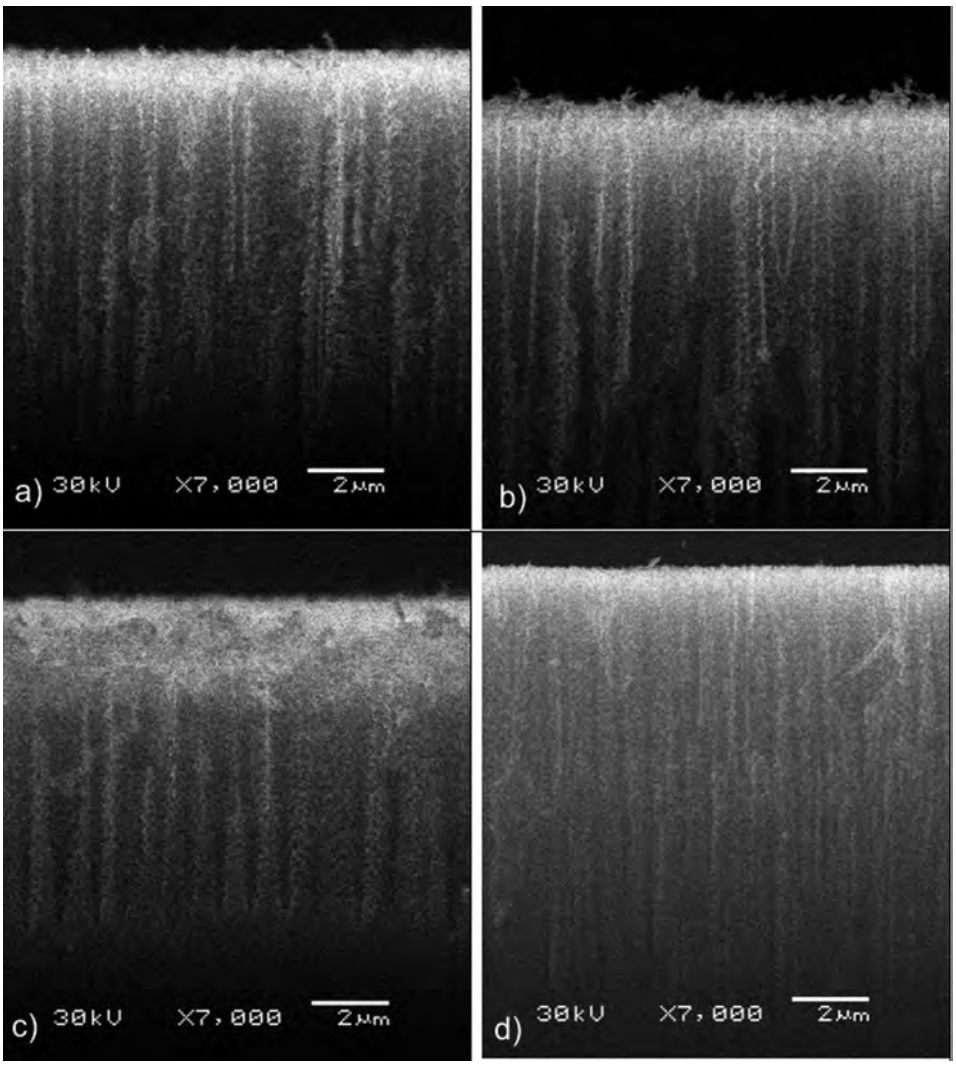

Fig. 1. SEM images of cleavages of porous silicon samples obtained in single and two-stage etching modes a) No. 1, j_a = 15 mA/cm^2; b) No. 2, j_a = 50 mA/cm^2, c) No. 3, j_a = 50/15 mA/cm^2; d) No. 4, j_a = 15/50 mA/cm^2

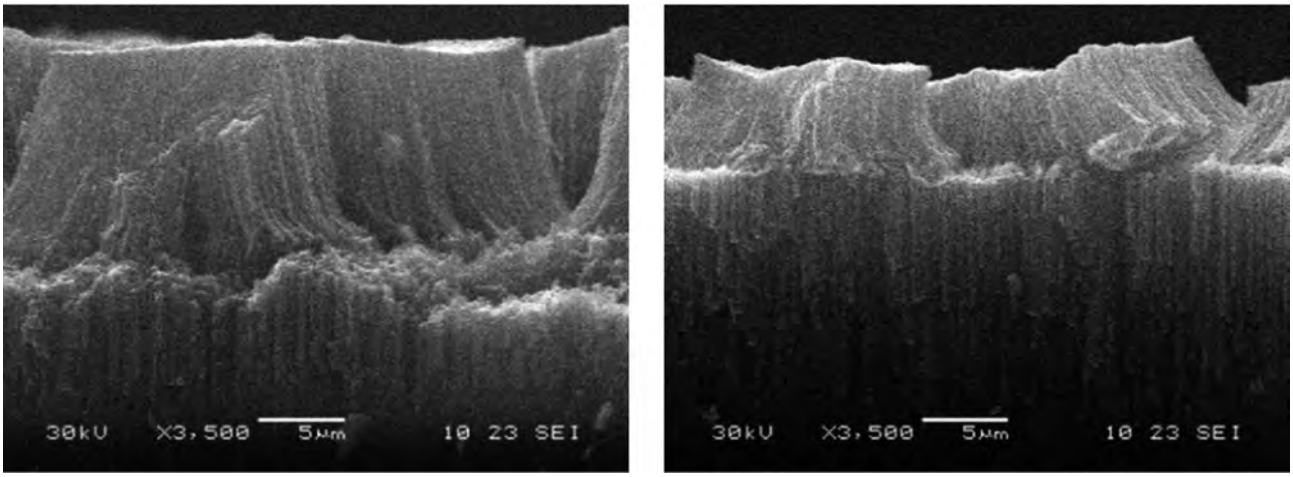

Fig. 2. SEM images of cleavages of mesoporous silicon samples obtained in two-stage etching modes: a) No. 208, j_a =50/15 mA/cm^2; b) No. 207, j_a = 15/50 mA/cm^2 [8]

15 μ, while the thickness of the porous layer of sample No. 2 obtained with the current density of j = 50 mA/cm^2 was ~ 25 μ (Fig. 1). The average diameter of the main type of pores in the samples was 150-200 nm.

The smaller thickness of the macroporous silicon layer, as compared to the mesoporous silicon, as well as the absence of stratification in the surface layer, can be explained by the lower concentration of hydrofluoric acid in the ECE solution. Taking into account the etching time of 10 min, the etching rate of the porous layer was ~ 1.5 μ/min and 2.5 μ/min for samples No. 1 and No. 2 respectively, and it increased by 1.5 times with more than a threefold increase in the current density (similar to mesoporous silicon). The average size of vertical pores in mesoporous silicon was ~ 50–100 nm.

As for samples No. 3 and 4 (fig. 1c, d), obtained using two-stage modes of changing the anodic current density, that is in the modes of decreasing (j = 50/15 mA/cm^2) and increasing (j = 15/50 mA/cm^2) the ECE current density, the thickness of the porous layer of the samples was ~ 15 μ and ~ 18 μ respectively. An analysis of the images of sample cleavages indicates that the depth of the boundary between the layers of the structure, similar to mesoporous silicon, is determined by the primary ECE mode [11].

3.2. IR spectra of macroporous and mesoporous silicon

To obtain information on the composition of the chemical bonds in porous layers, all samples of macroporous and mesoporous silicon were studied using IR spectroscopy.

Fig. 3 presents the IR spectra of ATR showing the effect of an increase in the ECE current density and changes in the sequence of values of currents during a two-stage ECE on the composition of chemical bonds of macroporous silicon samples. A band of 1000-1200 cm^{-1} corresponding to Si–O–Si bonds and an intensity mode corresponding to the vibrations of Si–Si bonds (616 cm^{-1}) are observed on these IR spectra. The Si–O–Si band is shown most clearly and intensively in sample No. 4 obtained in a two-stage ECE mode, j_a = 15/50 mA/cm^2. In addition, a low-intensity features appear in the IR spectra in the regions of ~ 900 cm^{-1} and 2060–2120 cm^{-1} which are typical for various configurations of the Si–H_x and O_x–SiH bonds. The presented results correlate well with the previously obtained results for different single layer structures of porous silicon [9].

Fig. 4 shows the IR spectra of ATR of mesoporous silicon samples obtained in the modes of single-stage and two-stage etching with a different sequence of changes in the ECE current values. At first glance, these spectra stand out due to their significantly higher intensity and pronounced structuredness of all modes that were barely visible in the IR spectra of the macroporous silicon samples presented in Fig. 3. The most intensive and clearly structured modes in the spectra of mesoporous silicon are those in the region of 400–1200 cm^{-1} which are typical for this material [9] and correspond to the vibrations of the following bonds: Si–Si (616

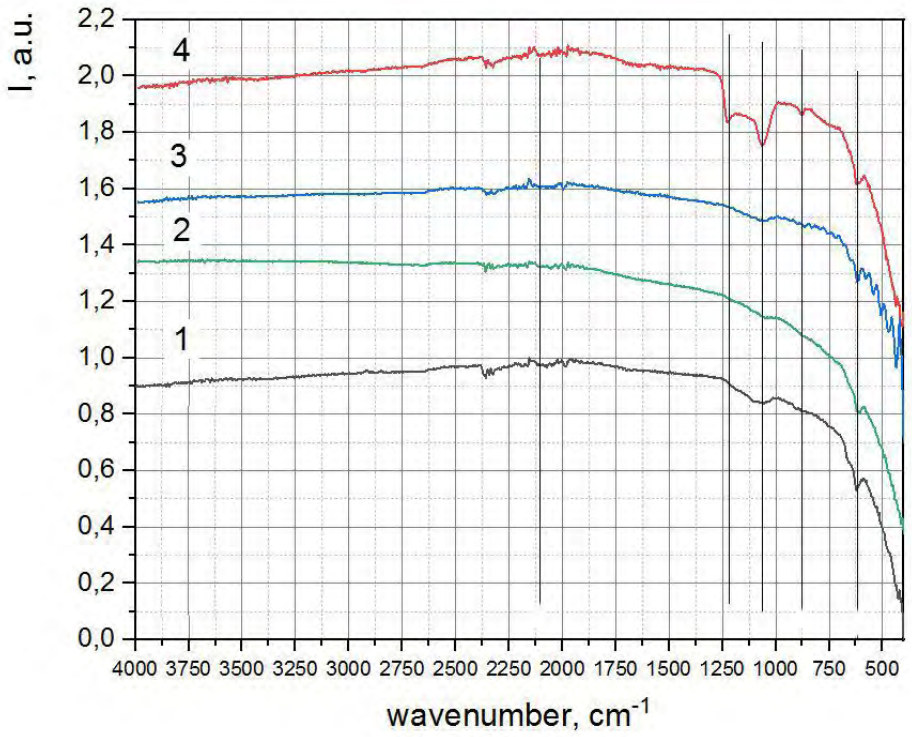

Fig. 3. IR-spectra of macroporous silicon samples obtained in single and two-stage etching modes: a) No. 1, j_a = 15 мА/см^2; b) No. 2, j_a = 50 мА/см^2, c) No. 3, j_a = 50/15 мА/см^2; d) No. 4, j_a = 15/50 мА/см^2

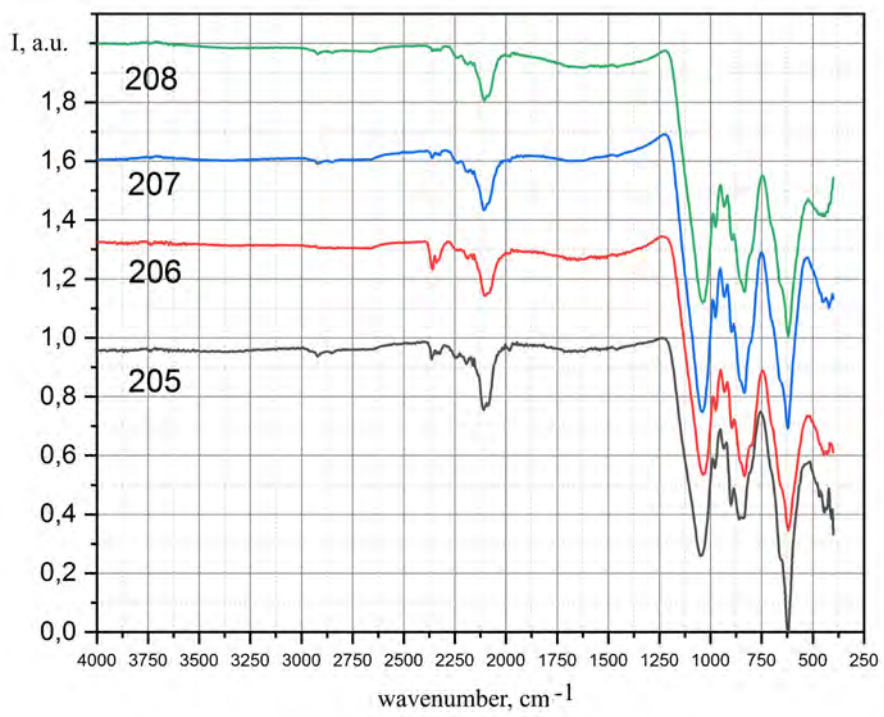

Fig. 4. IR-spectra of mesoporous silicon samples obtained in single and two-stage etching modes: No. 205, j_a = 15 mA/cm^2; No. 206, j_a = 50 mA/cm^2; No. 207, j_a = 15/50 mA/cm^2; No. 208, j_a = 50/15 mA/cm^2

cm^{-1}), Si–H$_x$ (664, 906, 2100–2250 cm^{-1}), Si–O–Si (490, 1060–1170 cm^{-1}), O$_2$– Si–OH (~ 830 cm^{-1}), O$_3$–SiH (880 cm^{-1}).

In addition, there are noticeable bands in the region of 2060–2120 cm^{-1} on the spectra of the samples. These bands are typical for various configurations of Si–H$_x$ and O$_x$–SiH$_y$ bonds as well as adsorbed CO$_2$ (2360 cm^{-1}). The presence of these bonds indicates a significantly greater sorption capacity of mesoporous silicon with a larger specific surface area of smaller pores as compared to macroporous silicon.

While comparing mesoporous samples obtained in single-stage modes (No. 205 and No. 206), it should be noted that an increased ECE current density leads to an increase in relative intensity of absorption bands in the regions of 750–900 cm^{-1} (Si–H$_x$, O$_2$–Si–OH, and O$_x$–SiH$_y$ bonds) and the 1000–1200 cm^{-1} band corresponding to Si–O–Si bonds. In combination with the SEM data, this indicates an increase in the specific surface area of the porous layer S_{sp} for the samples obtained with a higher ECE current density. At the same time, increased S_{sp} contributes to a more active interaction of the material with the environment, which leads to stronger oxidation of the porous layer and adsorption of hydrogen and hydroxyl groups on it [8, 9].

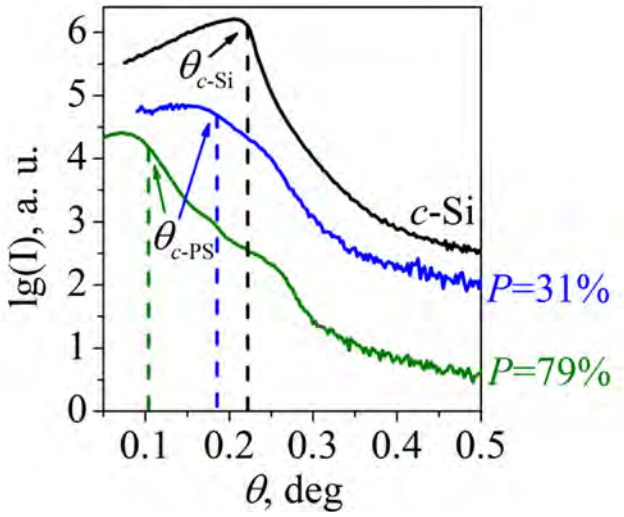

Fig. 5. XRR profiles of the samples of macroporous (the blue curve) and mesoporous silicon (the green curve) and single-crystal silicon substrate *c*-Si. The dotted lines indicate the positions of the critical angles of total external reflection

A similar situation is observed when changing the sequence of changes in the current values during ECE. The IR spectrum of sample No. 207 obtained in a two-stage mode j_a = 15/50 mA/cm^2 shows more intensive, as compared to the spectrum of a single-stage sample No. 205 (obtained in the mode with minimal current density j_a = 15 mA/cm^2), absorption bands 50–900 cm^{-1} and 1000–1200 cm^{-1} corresponding to Si–O–Si, Si–H$_x$, O$_2$–Si–OH, and O$_x$–SiH$_y$ bonds. These modes are less intensive as compared to the spectrum of the mode obtained with maximum ECE current density (No. 208, j_a = 50/15 mA/cm^2) in a two-stage mode.

Thus, a comparative analysis of the relative intensity and fine structure of vibrational modes of IR spectra indicated a significantly more developed specific pore surface and greater sorption capacity of mesoporous silicon as compared to macroporous silicon.

3.3. X-ray reflectivity

Fig. 5 shows XRR reflectograms of mesoporous and macroporous silicon samples (No. 206 and No. 2) obtained in single-stage modes and a silicon substrate of single-crystal silicon Si (100) on which porous layers were formed. The results show that the intensity of the XRR curves begins to decrease significantly after passing the critical angle θ_c of the total external reflection (TER) of X-ray radiation where the intensity of the reflected X-ray radiation is reduced by half. In this case, the values of critical angles of TER for the three studied samples were markedly different. The critical angle of TER for a single-crystal silicon wafer *c*-Si is $\theta_{c\text{-Si}}$ = 0.223°, which correlates well with theoretical calculations (0.226°). At the same time, the values of critical angles for macroporous and mesoporous silicon are considerably lower: $\theta_{c\text{-PS}}$ = 0.186° and $\theta_{c\text{-PS}}$ = 0.105° respectively.

The porosity (*P*) of the surface layer of the samples can be evaluated using ratio (1) presented in [12]:

$$P(\%) = \left[1 - \left(\theta_{c-\text{PS}} / \theta_{c-\text{Si}}\right)^2\right] \times 100, \quad (1)$$

where $\theta_{c\text{-Si}}$ is the critical angle of TER of single-crystal silicon c-Si, $\theta_{c\text{-PS}}$ is a critical angle of TER of the porous layer of the samples of macroporous or mesoporous silicon. In accordance with ratio (1), the value of porosity of mesoporous

silicon P = 79 % is 2.5 times higher than the corresponding value of macroporous silicon P = 31 %.

The measurements of the photoluminescence of porous silicon samples using the technique described in [13] showed the absence of PL in a sample of macroporous silicon with porosity of 31 % (sample No. 2) and the presence of typical PL for sample No. 206 of mesoporous silicon with porosity of P = 79 %. This correlates with the results of previous studies, according to which porous silicon begins to luminesce with the value of porosity P higher than 50 % [13, 14].

4. Conclusions

The paper presented the results related to the development of techniques or the two-stage formation of multilayer structures of porous silicon with various porosity and various sizes of pores.

Using scanning electron microscopy, it was shown that with the two-stage growth of porous silicon layers, the depth of the boundary between the layers of the structure was determined by the primary mode of electrochemical etching, while the total layer thickness increased with an increase in the ECE current density.

The average diameter of the main type of pores in the samples of macroporous silicon was 150–200 nm, while the average diameter vertical pores in mesoporous silicon was two-three times less, ~ 50–100 nm.

Comparative analysis of the relative intensity and fine structure of vibrational modes of IR spectra indicated that multilayer samples of macroporous silicon were less oxidated as compared to the samples of mesoporous silicon and that the surface of pores contained fewer bonds of the Si–OH and Si–H type.

The porosity of the surface layer of mesoporous silicon P = 79 % determined by the X-ray reflectivity was 2.5 times higher than the corresponding value of macroporous silicon P = 31 %, which correlated well with the significantly more developed specific surface of pores and greater sorption capacity of mesoporous silicon as compared to macroporous silicon.

Conflict of interests

The authors declare that they have no known competing financial interests or personal relationships that could have influenced the work reported in this paper.

References

1. Pacholski C. Photonic crystal sensors based on porous silicon. *Sensors*. 2013;13(4): 4694–4713. https://doi.org/10.3390/s130404694

2. Harraz F. A. Porous silicon chemical sensors and biosensors: A review. *Sensors and Actuators B: Chemical*. 2014;202: 897–912. https://doi.org/10.1016/j.snb.2014.06.048

3. Qian M., Bao X. Q., Wang L. W., Lu X., Shao J., Chen X. S. Structural tailoring of multilayer porous silicon for photonic crystal application. *Journal of Crystal Growth*. 2006;292(2): 347–350. https://doi.org/10.1016/j.jcrysgro.2006.04.033

4. Len'shin A. S., Kashkarov V. M., Turishchev S. Yu., Smirnov M. S., Domashevskaya E. P. Effect of natural aging on photoluminescence of porous silicon. *Technical Physics Letters*. 2011;37(9): 789–792. https://doi.org/10.1134/S1063785011090124

5. Kheifets L. I., Neimark A. B. *Multiphase processes in porous media*. Moscow: Khimiya Publ.; 1982. 320 p. (In Russ.)

6. Canham L. *Handbook of porous silicon*. Switzerland: Springer International Publishing; 2014. 733 p.

7. Zimin S. P. Porous silicon – material with new properties. *Soros Educational Journal*. 2004;8(1): 101–107. Available at: http://window.edu.ru/resource/217/21217/files/0401_101.pdf_(In Russ., abstract in Eng.)

8. Seredin P. V., Lenshin A. S., Goloshchapov D. L., Lukin A. N., Arsentyev I. N., Bondarev A. D., Tarasov I. S. Investigations of nanodimensional Al_2O_3 films deposited by ion-plasma sputtering onto porous silicon. *Semiconductors*. 2015;49(7): 915–920. https://doi.org/10.1134/S1063782615070210

9. Seredin P. V., Lenshin A. S., Mizerov A. M., Leiste H., Rinke M. Structural, optical and morphological properties of hybrid heterostructures on the basis of GaN grown on compliant substrate por-Si(111). *Applied Surface Science*. 2019;476: 1049–1060. https://doi.org/10.1016/j.apsusc.2019.01.239

10. Seredin P. V., Leiste H., Lenshin A. S., Mizerov A. M. Effect of the transition porous silicon layer on the properties of hybrid GaN/SiC/por-Si/Si(111) heterostructures. *Applied Surface Science*. 2020;508(145267): 1–14. https://doi.org/10.1016/j.apsusc.2020.145267

11. Lenshin A. S., Barkov K. A., Skopintseva N. G., Agapov B. L., Domashevskaya E. P. Influence of electrochemical etching modes under one stage and two Stage formation of porous silicon on the degree of oxidation of its surface layer under natural conditions. *Kondensirovannye sredy i mezhfaznye*

granitsy = Condensed Matter and Interphases. 2019;21(4): 534–543. https://doi.org/10.17308/kcmf.2019.21/2364 (In Russ., abstract in Eng.)

12. Buttard D., Dolino G., Bellet D., Baumbach T., Rieutord F. X-ray reflectivity investigation of thin p-type porous silicon layers. *Solid State Communications*. 1998;109(1): 1–5. https://doi.org/10.1016/S0038-1098(98)00531-6

13. Lenshin A. S., Seredin P. V., Agapov B. L., Minakov D. A., Kashkarov V. M. Preparation and degradation of the optical properties of nano-, meso-, and macroporous silicon. *Materials Science in Semiconductor Processing*. 2015;30: 25–30. https://doi.org/10.1016/j.mssp.2014.09.040

14. Ksenofontova O. I., Vasin A. V., Egorov V. V., Bobyl' A. V., Soldatenkov F. Yu., Terukov E. I., Ulin V. P., Ulin N. V., Kiselev O. I. Porous silicon and its applications in biology and medicine. *Technical Physics*. 2014;59(1): 66–77. https://doi.org/10.1134/S1063784214010083

Information about the authors

Alexander S. Lenshin, PhD in Physics and Mathematics, Senior Researcher, Department of Solid State Physics and Nanostructures, Voronezh State University, Voronezh, Russian Federation; e-mail: lenshinas@phys.vsu.ru. ORCID iD: https://orcid.org/0000-0002-1939-253X.

Anatoly N. Lukin, PhD in Physics and Mathematics, Associate Professor, Department of Solid State Physics and Nanostructures, Voronezh State University, Voronezh, Russian Federation; e-mail: ckp_49@mail.ru. ORCID iD: https://orcid.org/0000-0001-6521-8009.

Yaroslav A. Peshkov, PhD student, Department of Solid State Physics and Nanostructures, Voronezh State University, Voronezh, Russian Federation; e-mail: Tangar77@mail.ru. ORCID iD: https://orcid.org/0000-0002-2918-3926.

Sergey V. Kannykin, PhD in Physics and Mathematics, Associate Professor, Department of Materials Science and the Industry of Nanosystems, Voronezh State University, Voronezh, Russian Federation; e-mail: svkannykin@gmail.com. ORCID iD: https://orcid.org/0000-0001-8756-5722.

Boris L. Agapov, PhD in Technical Science, Centre for Collective Use of Scientific Equipment, Voronezh State University, Voronezh, Russian Federation; e-mail: b.agapov2010@yandex.ru.

Pavel V. Seredin, DSc in Physics and Mathematics, Head of the Department of Solid State Physics and Nanostructures, Voronezh State University, Voronezh, Russian Federation; e-mail: paul@phys.ru. ORCID iD: https://orcid.org/0000-0002-6724-0063.

Evelina P. Domashevskaya, DSc in Physics and Mathematics, Full Professor, Department of Solid State Physics and Nanostructures, Voronezh State University, Voronezh, Russian Federation; e-mail: ftt@phys.vsu.ru. ORCID iD: https://orcid.org/0000-0002-6354-4799.

All authors have read and approved the final manuscript.

Received 5 February 2021; *Approved after reviewing 15 February 2021*; *Accepted 15 March 2021; Published online 25 March 2021.*

Translated by Marina Strepetova
Edited and proofread by Simon Cox